

Implantable Glucose Biosensor with Enhancing Electron Transfer - Nanocomposite Functional Layers

Xianying Zhang, Qiyu Wang*

Institute of Physics, Chinese Academy of Sciences, Beijing 100190, China

*E-mail: qywang10@iphy.ac.cn

Received: 22 September 2020 / Accepted: 11 November 2020 / Published: 30 November 2020

A nanocomposite of ferrocenecarboxylic acid (FcA), graphene oxide (GO), chitosan (CS) and glucose oxidase (GOD) has been developed and used as the functional component of a needle-type implantable glucose biosensor. GOD was successfully immobilized in a single step without any crosslinking agents; and the enzymatic function and specificity was preserved. The biosensor morphology was characterized by scanning electron microscopy (SEM), and the functional properties were examined electrochemically. We showed that our glucose biosensor exhibited a fast response with high reproducibility and stability. A linear response to glucose - which was mostly undisturbed by common interfering species - was obtained between glucose concentrations between 0.01 to 10 mM. The detection limit and sensitivity of our biosensor were 19 μM and 8 $\text{mA cm}^{-2}\text{mM}^{-1}$ ($S/N = 3$), respectively.

Keywords: ferrocenecarboxylic acid, graphene oxide, chitosan, glucose oxidase, needle-type biosensor

1. INTRODUCTION

Diabetes mellitus is a widespread disease which causes death and disability. According to the World Health Organization (WHO), the rate of morbidity is increasing[1], such that between 2017 and 2045, the number of patients globally is expected to increase from 451 million to 693 million [2, 3]. In 2017, approximately 5 million deaths worldwide were attributable to diabetes in the 20-99 years age range[3]. Specialists predict that diabetes will become the world's seventh largest cause of death by 2030. Hence, the development of high-performance glucose detection technology is essential for monitoring diabetes mellitus; and currently, biosensors have been shown to offer the most promising advancements[4].

At present, most commercialized glucose biosensors are based on electrochemical enzyme-based sensors, which combine the substrate specificity of enzymes with electrochemical transduction methods. Accordingly, highly selective, sensitive, low-cost and simple instrumentation is obtained[5]. To achieve

this, the enzyme must be immobilized onto electrode surfaces; and efficient methods which enable the electrochemical reaction while maintaining their bioactivities are essential[6-8]. This has been achieved by either covalently binding enzymes onto substrate surface or incorporating enzymes into different matrices[9-11]. The incorporation of enzymes into a matrix is advantageous over immobilization methods as it maximizes enzyme loading while protecting the enzyme from the surrounding environment. Additionally, electron transfer between the enzymes and electrode must be optimized since the active sites of the enzymes are usually deeply embedded inside the protein shell and electron transfer is often inefficient[12].

In order to address these two issues, we used a homogeneous ferrocenecarboxylic acid—graphene oxide-chitosan/glucose oxidase (FcA-GO-CS/GOD) composite membranes as a platform for the fabrication of glucose biosensor. Chitosan (CS), obtained from the partial deacetylation of chitin[13], is a promising biopolymer matrix material for immobilizing enzymes due to its excellent film-forming ability, good adhesion, high permeability towards water, non-toxicity, excellent biocompatibility, high mechanical strength and ease of chemical modifications[14-20]. However, its electron transfer efficiency is very low, and must be enhanced with a covalently-bound redox mediator[21]. For this, a carboxylated derivative of ferrocene (FcA), which is a well-known mediator with reversibility, the ability to be regenerated at low potential, and stable redox states, shows great promise[22-24]. Finally, the electron transport could be enhanced by compositing FcA and CS with graphene, a two-dimensional carbon nanomaterial[25-27]. Graphene has recently attracted tremendous attention because of its unique nanostructure and many extraordinary properties, such as exceptional conductivity, excellent thermal and chemical stability, outstanding mechanical flexibility, and environmental friendliness[28-32]. Therefore, it is a remarkable candidate matrix material for electrochemical biosensors.

Here, needle-type implantable glucose biosensors were prepared using a nanocomposite comprising CS, FcA and GO. The simple, one-pot fabrication process entails the initial mixing of ferrocenecarboxylic acid (FcA), graphene oxide (GO) and chitosan (CS) were mixed together, followed by the addition and mixing with glucose oxidase (GOD) without any cross linking agents or modifiers to achieve the FcA-GO-CS/GOD nanocomposite. Finally, a needle-type implantable glucose biosensor was prepared by fixing a nanocomposite film to the needle-type electrodes. Most importantly, our prepared nanocomposite exhibited superior performance for glucose detection than competing State-of-the-Art materials, boasting a low detection limit, a wide detection range, high selectivity, excellent sensitivity, and good stability.

2. EXPERIMENTAL

2.1. Apparatus

Scanning electron microscopy (SEM) was used to characterize the composite morphology (Electron Microscopy Inc., Cambridge, U.K.). All electrochemical experiments were carried out with a CHI 650D model electrochemical workstation (Shanghai, Chenhua Co., China). A three-electrode cell was used with a modified glassy carbon electrode (GCE) or the fabricated needle-type platinum

electrodes as the working electrode, a saturated calomel electrode (SCE) as the reference electrode and a platinum wire as the counter electrode. Amperometric measurements were performed in 0.1 M phosphate buffer saline (PBS, pH 7.4) under gentle stirring at room temperature. The electrolyte was bubbled with high-purity (99.999%) N₂ for 15 min. Ultrasonic Cleaner KQ-800KDE (Kunshan Co. Ltd, China) was used to clean samples during preparation.

2.2. Reagents and materials

Graphite was purchased from Alfa Aesar Co (USA). Chitosan (CS, 200-400 mPa·s), ferrocenecarboxylic acid (FcA, 98%), glucose oxidase (GOD, EC 1.1.3.4, 100 U/mg) were purchased from Sigma-Aldrich. D-(+)-glucose, uric acid (UA), L-ascorbic (AA) and dopamine hydrochloride (DA) were purchased from Beijing Chemical Reagent (Beijing, China), All other chemicals used in this investigation were of analytical grade (99.9%). Phosphate buffer solution (PBS, 0.1 M, pH 7.4) was used as a supporting electrolyte for all electrochemical measurements. Deionized water was obtained from an in-house Millipore Milli-Q system (18.2 MΩ cm at 25 °C). All experiments were performed at room temperature (25 ± 1 °C).

2.3. Production of FcA-CS-GO/GOD nanocomposite precursor.

Graphene oxide was prepared according to our previous work[33]. GO and FcA were dispersed into water by ultrasonication for 2 h in separate vials to achieve homogeneous GO suspension (5 mg·mL⁻¹) and FcA suspension (0.075 M), respectively. GOD was dissolved in 0.1 M PBS (pH 7.4) by stirring to produce a 10 mg/mL GOD solution. 1.5 g CS was added into 98.5 g deionized water followed by 1 mL acetic acid, and then stirred for 2 h at room temperature. 60 μL FcA suspension (0.075 M), 3 μL GO suspension (5 mg/mL) and 60 μL CS solution (1.5%) were mixed with ultrasonication for 2 h to produce FcA-CS-GO precursor mixture. Finally, 60 μL 10 mg/mL GOD solution was added, and the mixture was stirred 30 min to yield a FcA-CS-GO/GOD nanocomposite precursor.

2.4. Fabrication of FcA-CS-GO/GOD nanocomposite-modified electrode.

The GCEs were carefully polished with alumina polishing powder and washed sequentially with ethanol and deionized water by ultrasonication for 3 min. The GCE surface was coated with 10 μL FcA-CS-GO/GOD nanocomposite precursor and dried at room temperature. 5 μL of Nafion solution (0.5% in ethanol) was then dropped onto the surface of FcA-CS-GO/GOD nanocomposite-modified GCE. Prior to testing, the GCEs were rinsed with deionized water for several times to remove any loosely attached nanocomposite. The test solution was N₂-saturated PBS (0.1 M, pH 7.4).

2.5. Fabrication of FcA-CS-GO/GOD nanocomposite-modified needle-type electrode

The needle-type electrodes were steel needles coated with electrodeposited platinum. A silane film was precoated onto the surface of the needle-type electrode, and dried in vacuum for 8 h. The electrode was then covered with the FcA-CS-GO/ GOD nanocomposite and silane in tune, and dried for 15 h. The biosensor was then completed by adding a final polyurethane membrane onto the electrode surface.

3. RESULTS AND DISCUSSION

3.1. Morphology characterization of the needle-type glucose biosensor

SEM analysis showed that the most significant feature was homogeneous dispersion of the 20-50 nm diameter, electrodeposited Pt particles on the electrode surfaces (Fig. 1a). This provides an excellent platform for the proceeding deposition steps. Pt nanoparticle deposition was advantageous because it increased the electrode activity by increasing the surface area and thereby increased the availability of a greater number of active sites in the immobilized enzyme[34, 35]. Additionally, Pt nanoparticles are also known to be excellent catalysts for the breakdown of hydrogen peroxide[36], which could effectively convert chemical signals into electrical signals and transmit to the detection system. The morphology of the overlaid FcA-CS-GO/GOD nanocomposite was generally smooth but folded into large wrinkles, and thus the underlying surface topography was lost (Fig. 1b). However, the wrinkles, which formed during drying, would be expected to increase the activity of the electrode by again increasing the surface area, especially compared to a flat surface. Finally, SEM analysis of the morphology of the polyurethane diffusion limiting membrane deposited on the surface of the FcA-CS-GO/GOD showed the formation of many pores which were distributed across the electrode surface. It comprises the outermost layer of diffusion limit film, which is produced by polyethylene glycol (PEG) and potassium chloride (KCl) aqueous solution, and is designed to change the hydrophilicity of the glucose biosensor. Corresponding CCD microscope images (inset) showed the change on the surface during each step of preparation process of the biosensor (Fig. 1).

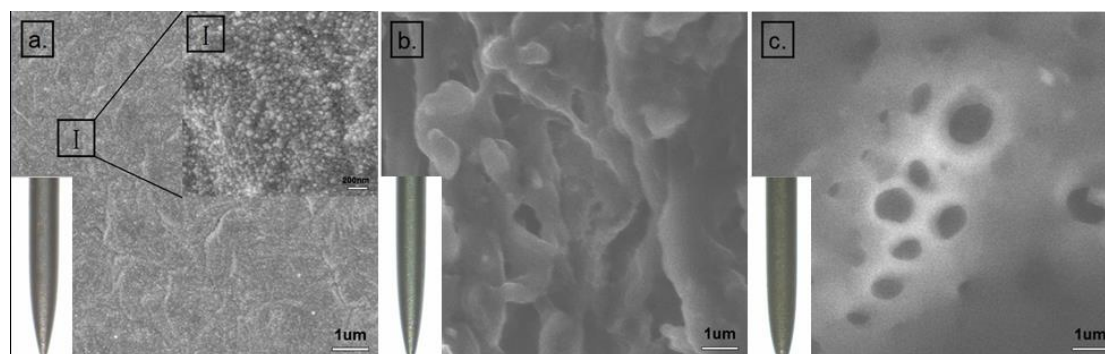


Figure 1. SEM images of the morphologies of the Pt-plated steel needle (a) before coating and (b) after coating with FcA-CS-GO/GOD and (c) after coating with the polyurethane diffusion limited membrane. Corresponding CCD microscope images are located in the lower left corner of each image.

3.2. Electrocatalytic performance of the FcA-CS-GO/GOD film-modified electrode

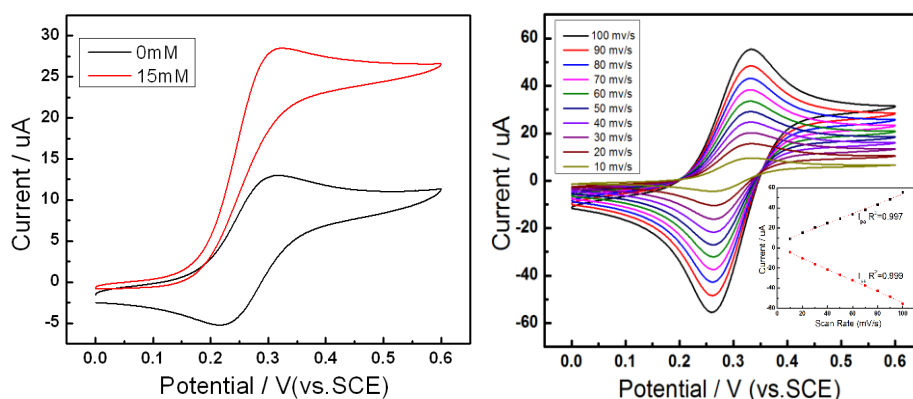


Figure 2. Cyclic voltammograms of the GOD/FcA-GO-CS film-modified electrode (a) in the absence (black) and presence (red) of 15.0 mM glucose in N_2 -saturated PBS (pH = 7.4). Scan rate = $100 \text{ mV}\cdot\text{s}^{-1}$. (b) in N_2 -saturated PBS (0.1 M, pH 7.4) at 10, 20, 30, 40, 50, 60, 70, 80, 90 and $100 \text{ mV}\cdot\text{s}^{-1}$ (from internal to external). The inset is the plot of anodic and cathodic peak current versus scan rate.

Cyclic voltammetry (CV) studies[14, 15, 34] were conducted using a GOD/FcA-CS-GO-modified glassy carbon electrode (GCE) as the working electrode to characterize the electrochemical performance (Fig. 2). In the absence of glucose, a standard, reversible electrochemical behavior of FcA was observed, but in the presence of 15 mM glucose, the anodic peak current increased dramatically (Fig. 2a). This was attributed to the oxidation of glucose by GOD in the electrode surface. This also confirmed that GOD retained its bioactivity after mixing with FcA-CS-GO. By appreciating the cooperative redox behavior of both the GOD and the FcA[12-14, 21, 24], a mechanism was proposed[37-40]. Firstly, glucose was oxidized by GOD to gluconolactone, which in turn reduced the enzyme from GOD(ox) to GOD(red). Secondly, the GOD(red) was oxidized by the electron mediator FcA back to its original state, GOD(ox), at an amperometric catalytic anodic current. CVs of the GOD/FcA-GO-CS were also run under the same conditions but at different scan rates in the range of 10– $100 \text{ mV}\cdot\text{s}^{-1}$ (Fig. 2b). We clearly observed a pair of reversible redox peaks located at 0.33 V and 0.27 V vs. saturated calomel electrode (SCE), which was indicative of the electron transfer from FcA on the electrode surface. Further analysis of the CV data showed that the cathodic and anodic peak currents increased linearly as the scan rate increased, which suggested that the electrochemical reaction of the GOD/FcA-GO-CS film-modified electrode was a diffusion-controlled process (Fig. 2b).

3.3. Electrocatalytic behavior of the FcA-CS-GO/ GOD film-modified needle-type glucose biosensor.

The typical amperometric response[38, 40] of the GOD/FcA-GO-CS film-modified a needle-type glucose biosensor was assessed with the successive addition of glucose into the electrolyte under an applied potential of 0.33 V (Fig. 3). Our data showed that the biosensor reached 95% of the steady-state current within 3 s. This rapid response to changes in glucose concentration was attributed to the presence of the electron transfer mediator FcA[13, 22]. The amperometric response increased linearly

with glucose concentration between 0.01 and 10 mM (Fig. 3). We determined a detection limit of 19 μM and a sensitivity of approximately $8 \mu\text{A cm}^{-2}\text{mM}^{-1}$ ($S/N = 3$). A comparison of the electrochemical performances of GOD/FcA-GO-CS with other enzymatic glucose sensors (Table 1). 91.2% of the original sensitivity [41] of the biosensor was maintained after 4 consecutive uses, which was indicative of good stability and reusability (Fig. 4).

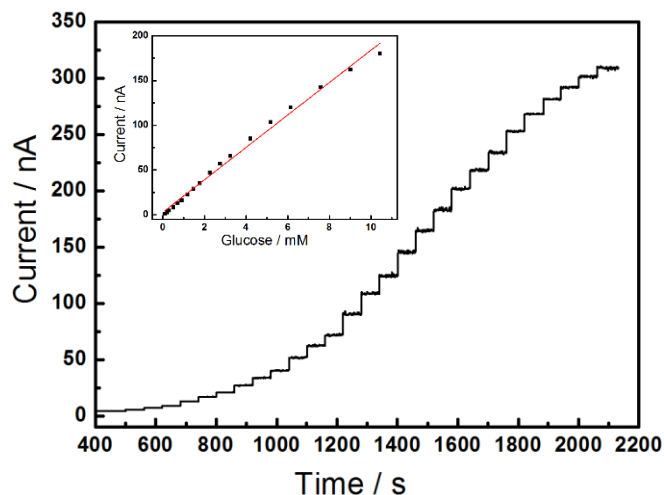


Figure 3. Amperometric response of the GOD/FcA-GO-CS film-modified a needle-type glucose biosensor at an applied potential +330 mV with the successive addition of glucose in a stirred N_2 -saturated 0.1 M PBS (pH = 7.4).

Table 1. A comparison of the electrochemical performances of GOD/FcA-GO-CS with other enzymatic glucose sensors

Electrode	Linear range (mM)	Limit of detection (μM)	Sensitivity ($\mu\text{A mM}^{-1}\text{cm}^{-2}$)	References
GOD/rGO-TEPA/PB	0.1-25	25	-	[39]
Fe_3O_4 -CS-CD/MWCNTs/GOD/GCE	0.04-1.04	19.30	23.59	[38]
GOD/AuNPs/GO/MWCNTs	0.3-2.1	4.8	29.72	[42]
ZnO rods/CS/GOD/GCE	0.01-0.04	-	-	[43]
GOD- SiO_2 /Lig/CPE	0.5-9	145	-	[37]
GOD-CS-IL-PB-Pt	0.01-4.2	5	37.8	[44]
GOD/Naf/ MnO_2 -GNR/SPCE	0.1-1.4	0.05	56.32	[45]
GOD/AuNP/PANI/rGO/ NH_2 -MWCNTs	1-10	246	64	[40]
PANI-MMT/PtNPs/CS-GOD	0.01-1.94	0.1	-	[41]
GOD/FcA-GO-CS	0.01-10	19	8	This work

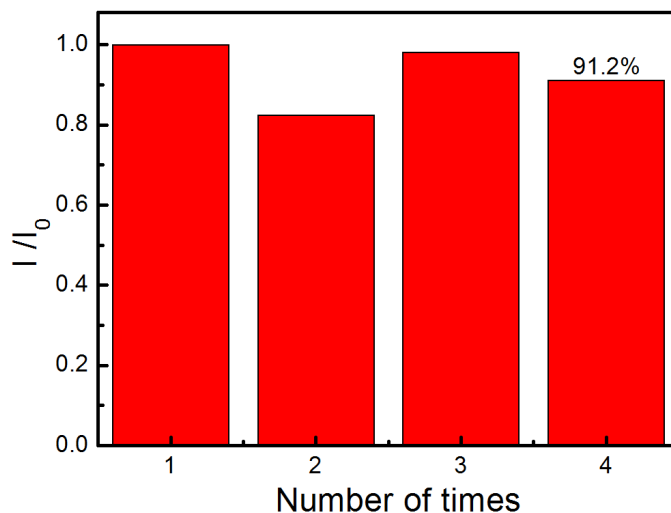


Figure 4. Stability of the GOD/FcA-GO-CS film-modified a needle-type glucose biosensor at an applied potential of +330 mV in a stirred N_2 -saturated 0.1 M PBS (pH = 7.4) with the addition of 1 mM glucose.

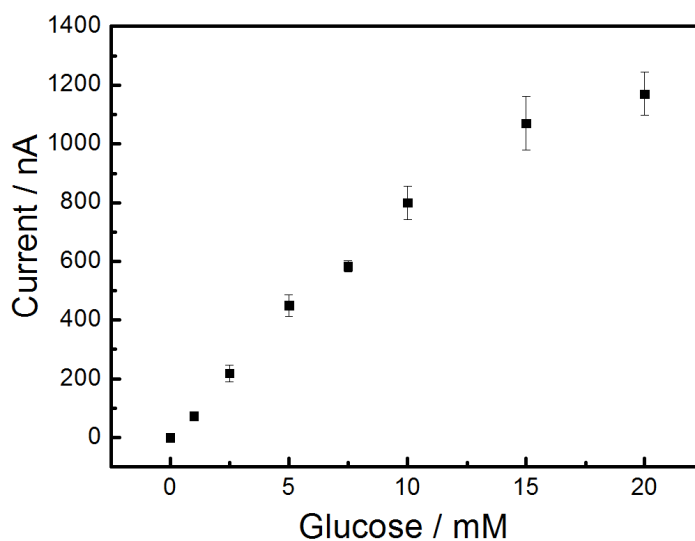


Figure 5. Amperometric response of the GOD/FcA-GO-CS film-modified needle-type glucose biosensors at an applied potential +330 mV to different concentrations of glucose in 0.1 M PBS (pH = 7.4). Error bars are equivalent to a standard deviation ($n = 3$).

In order to study the reproducibility, three identical GOD/FcA-GO-CS nanocomposite-modified needle-type glucose biosensors were prepared and tested (Fig. 5). The amperometric response of each of the electrodes was obtained simultaneously using a specialist in-house, glucose biosensing detector in our laboratory which can test up to ten biosensors at the same time. The difference between the three biosensors, as shown by the error bars at each measurement, was very small, and suggested that our glucose biosensor could be suitable for mass production.

3.4. Interfering solutes

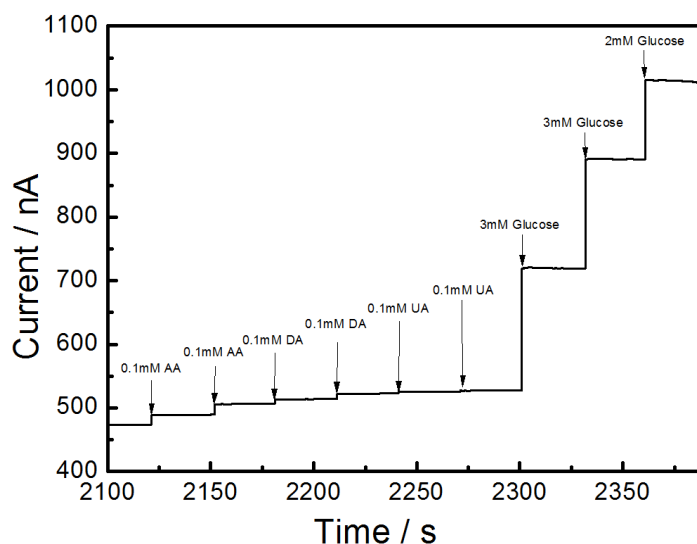


Figure 6. Interference test at an applied potential +330mV with 1mM glucose and other electroactive species including 0.1mM UA 、 0.1mM DA and 0.1mM AA in a stirred N₂-saturated 0.1M PBS (pH=7.4).

Finally, the selectivity[38, 41] of our GOD/FcA-GO-CS glucose biosensor was tested with interference studies. The change in current was recorded while different volumes of 0.1 mM AA solution, 0.1 mM DA solution, 0.1 mM UA solution were added to the glucose-enriched N₂-saturated 0.1M PBS electrolyte (Fig. 6). The responses caused by the interfering AA, DA and UA components were negligible compared to that caused by glucose. This suggested that the needle-type glucose biosensors were suitably selective for glucose detection under physiological conditions.

4. CONCLUSION

Needle-type implantable glucose biosensors based on GOD/FcA-GO-CS nanocomposite membranes were prepared using a simple one-pot method. The nanocomposite not only immobilized the enzyme while retaining its functionality, but also improved the efficiency of the electron transfer between GOD and the electrodes thanks to the mediated electron transfer. The high sensitivity and selectivity of the amperometric response of the biosensor was attributed to the synergy between GO, FcA and CS. Our needle-type implantable glucose biosensors exhibited a low detection limit 19 μ M, a wide detection range from 0.01 to 10 mM, high selectivity, excellent sensitivity, and good stability. We believe that the needle-type implantable glucose biosensors could be soon ready for commercial-scale production.

ACKNOWLEDGEMENTS

The authors would like to express their gratitude to EditSprings (<https://www.editsprings.com/>) for the expert linguistic services provided.

References

1. P. Zhang, X. Zhang, J. Brown, D. Vistisen, R. Sicree, J. Shaw and G. Nichols, *Diabetes Research and Clinical Practice*, 87(2010) 293.
2. L. Guariguata, D.R. Whiting, I. Hambleton, J. Beagley, U. Linnenkamp and J.E. Shaw, *Diabetes Research and Clinical Practice*, 103(2014) 137.
3. N.H. Cho, J.E. Shaw, S. Karuranga, Y. Huang, J.D. da Rocha Fernandes, A.W. Ohlrogge and B. Malanda, *Diabetes Research and Clinical Practice*, 138(2018) 271.
4. X. Cao, N. Wang, S. Jia and Y. Shao, *Analytical Chemistry*, 85(2013) 5040.
5. M. Li, X. Bo, Y. Zhang, C. Han and L. Guo, *Biosensors and Bioelectronics*, 56(2014) 223.
6. Y. Fu, P. Li, L. Bu, T. Wang, Q. Xie, J. Chen and S. Yao, *Analytical Chemistry*, 83(2011) 6511.
7. M.H. Freeman, J.R. Hall and M.C. Leopold, *Analytical Chemistry*, 85(2013) 4057.
8. U. Lad, G.M. Kale and R. Bryaskova, *Analytical Chemistry*, 85(2013) 6349.
9. X. Chen, J. Zhu, R. Tian and C. Yao, *Sensors and Actuators B: Chemical*, 163(2012) 272.
10. M. Şenel, C. Nergiz, M. Dervisevic and E. Çevik, *Electroanalysis*, 25(2013) 1194.
11. W. Zhao, Y. Ni, Q. Zhu, R. Fu, X. Huang and J. Shen, *Biosensors and Bioelectronics*, 44(2013) 1.
12. F. Qu, Y. Zhang, A. Rasooly and M. Yang, *Analytical Chemistry*, 86(2014) 973.
13. O. Yilmaz, D.O. Demirkol, S. Gulcemal, A. Kilinc, S. Timur and B. Cetinkaya, *Colloids and Surfaces B: Biointerfaces*, 100(2012) 62.
14. J.D. Qiu, R. Wang, R.P. Liang and X.H. Xia, *Biosensors and Bioelectronics*, 24(2009) 2920.
15. H. Wu, J. Wang, X. Kang, C. Wang, D. Wang, J. Liu, I.A. Aksay and Y. Lin, *Talanta*, 80(2009) 403.
16. J.-F. Wu, M.-Q. Xu and G.-C. Zhao, *Electrochemistry Communications*, 12(2010) 175.
17. K. Zhou, Y. Zhu, X. Yang, J. Luo, C. Li and S. Luan, *Electrochimica Acta*, 55(2010) 3055.
18. Y. Zhou, S. Liu, H.-J. Jiang, H. Yang and H.-Y. Chen, *Electroanalysis*, 22(2010) 1323.
19. J. Liu, S. Guo, L. Han, W. Ren, Y. Liu and E. Wang, *Talanta*, 101(2012) 151.
20. J. Liu, X. Wang, T. Wang, D. Li, F. Xi, J. Wang and E. Wang, *ACS Appl. Mater. Interfaces*, 6(2014) 19997.
21. J.D. Qiu, R.P. Liang, R. Wang, L.X. Fan, Y.W. Chen and X.H. Xia, *Biosensors and Bioelectronics*, 25(2009) 852.
22. S. Wang and D. Du, *Sensors and Actuators B: Chemical*, 97(2004) 373.
23. A. Escorcia and A.-A. Dhirani, *Journal of Electroanalytical Chemistry*, 601(2007) 260.
24. J.D. Qiu, W.M. Zhou, J. Guo, R. Wang and R.P. Liang, *Analytical Biochemistry*, 385(2009) 264.
25. K.S. Novoselov, A.K. Geim, S.V. Morozov, D. Jiang, Y. Zhang, S.V. Dubonos, I.V. Grigorieva and A.A. Firsov, *Science*, 306(2004) 666.
26. K.S. Novoselov, A.K. Geim, S.V. Morozov, D. Jiang, M.I. Katsnelson, I.V. Grigorieva, S.V. Dubonos and A.A. Firsov, *Nature*, 438(2005) 197.
27. A.K. Geim, *Science*, (2009) 324.
28. S. Guo, S. Dong and E. Wang, *ACS NANO*, (2010) 547.
29. M. Pumera, *Chemical Society Reviews*, 39(2010) 4146.
30. S. Guo and S. Dong, *Chem Soc Rev*, 40(2011) 2644.
31. J. Bai and X. Jiang, *Analytical Chemistry*, 85(2013) 8095.
32. S. Wu, Q. He, C. Tan, Y. Wang and H. Zhang, *Small*, 9(2013) 1160.
33. Q. Wang, X. Cui, J. Chen, X. Zheng, C. Liu, T. Xue, H. Wang, Z. Jin, L. Qiao and W. Zheng, *RSC Advances*, 2(2012) 6245.
34. X. Pang, D. He, S. Luo and Q. Cai, *Sensors and Actuators B: Chemical*, 137(2009) 134.
35. M. Jamal, J. Xu and K.M. Razeeb, *Biosensors and Bioelectronics*, 26(2010) 1420.
36. D. Zhai, B. Liu, Y. Shi, L. Pan, Yaqun Wang, W. Li, R. Zhang and Guihua Yu, *ACS NANO*, (2013) 3540.
37. A. Jędrzak, T. Rębiś, Ł. Klapiszewski, J. Zdarta, G. Milczarek and T. Jesionowski, *Sensors and Actuators B: Chemical*, 256(2018) 176.
38. L. Peng, Y. Luo, H. Xiong, S. Yao, M. Zhu and H. Song, *Electroanalysis*, (2020).

39. L. Cao, G.C. Han, H. Xiao, Z. Chen and C. Fang, *Analytica Chimica Acta*, 1096(2020) 34.
40. D. Maity, R.M. C and T.R. R, *Materials Science & Engineering C*, 105(2019) 110075.
41. H. Zheng, M. Liu, Z. Yan and J. Chen, *Microchemical Journal*, 152(2020) 104266.
42. Y. Yu, Z. Chen, S. He, B. Zhang, X. Li and M. Yao, *Biosensors and Bioelectronics*, 52(2014) 147.
43. S. Bagyalakshmi, A. Sivakami and K.S. Balamurugan, *Obesity Medicine*, 18(2020) 100229.
44. Y. Zhang, Y. Liu, Z. Chu, L. Shi and W. Jin, *Sensors and Actuators B: Chemical*, 176(2013) 978.
45. V. Vukojević, S. Djurdjić, M. Ognjanović, M. Fabián, A. Samphao, K. Kalcher and D.M. Stanković, *Journal of Electroanalytical Chemistry*, 823(2018) 610

© 2021 The Authors. Published by ESG (www.electrochemsci.org). This article is an open access article distributed under the terms and conditions of the Creative Commons Attribution license (<http://creativecommons.org/licenses/by/4.0/>).